

Control of the vertical motion of a hydrofoil vessel

Jangwhan Bai^a and Yonghwan Kim^{b*}

^a*Hyundai Maritime Research Institute, Hyundai Heavy Industries Co., Ulsan, Korea;* ^b*Department of Naval Architecture & Ocean Engineering, Seoul National University, Seoul, Korea*

(Received Received 17 May 2009; final version received 22 September 2009)

This paper presents the motion control of a fast ship equipped with fully submerged hydrofoils in following waves. The change of lift force produced by the orbital motion of fluid particles is included as a time-varying disturbance in the equation of coupled heave and pitch motions, and the corresponding state-space equation is derived. Three control algorithms, including proportional–integral–derivative (PID), linear quadratic regulator (LQR) and sliding mode controls are applied for regular and irregular wave conditions, and the subsequent motion responses are compared. Motion responses are also compared with existing experimental data to observe the effectiveness of each algorithm. In order to investigate the robustness of each control algorithm, systematic motion simulations are performed for various wavelengths and wave heights. PID control is easy to implement as is well known, however a poor performance is observed in irregular waves. LQR control predicts robust and stable motion and acceleration throughout all the simulations. Sliding mode control shows excellent performance particularly when the disturbance is known, despite its sensitivity to wave environments.

Keywords: ship motion control; control of hydrofoil; PID; LQR; sliding mode control

Introduction

Researches on controlling the longitudinal motion of fast ships using hydrofoil(s) were first introduced in the early 20th century. In the present study, primary interest is given to recent studies because a significant amount of computational and experimental results were developed in the 1990's.

To improve vertical motions in waves, Kang et al. (1993) and Lee and Rhee (2002) derived the linearised longitudinal equation of motion for foil catamarans. In the Kang et al. (1993) experiment with an optimal control, it was found that their catamaran model showed good performance in pitch motion in a wide range of frequencies, but not so much effectiveness in reducing heave motion. Lee and Rhee's research was focused on motion control in irregular sea conditions. They also tried to obtain the robustness of the control system using a frequency-domain analysis based on the assumption of regular ship motion. Their theoretical calculation and model tests verified that the assumption is valid, and the design technique ensures the robustness of the motion regulator.

Kim and Yamato (2004, 2005) tried to improve sea-keeping performance in following seas in which typical hydrofoil ships have bad performance. They applied an optimal control theory to a fully submerged hydrofoil model in still water and regular waves, but it was hard to get satisfactory results in regular waves possibly due to

the poor prediction of orbital motion of fluid particles in waves.

A state-space control-oriented time-domain model for ship motions was introduced by Ulusoy (2006). An interesting thing is that a discrete auto-regressive state-space model was developed using the linear seakeeping simulation method SWAN. In their study, the reliable motion analysis program called SWAN was coupled with LQ controllers to actively regulate the angle of attack of lifting appendages.

Chatzaklis and Sclavounos (2006) developed an optimal control law using modern state-space methods for the active motion control of high-speed hydrofoil vessels. The effectiveness of this method was demonstrated through stabilising the motion of vessels lacking a hydrostatic restoring mechanism in waves.

Most theoretical researches on ship motion control systems have applied LQ optimal control theory due to its remarkable performance. However, in reality, the proportional–integral–derivative (PID) controller has been leading the main stream of the motion control system. PID control is used in almost all real plants with some other supplementary method, e.g. gain scheduling. Recently, sliding mode control has been of interest because of its capacity for considering uncertainty of the vessel system (e.g. Kim 1997), but not as much as the attitude control system for aircraft.

*Corresponding author. Email: yhwankim@snu.ac.kr

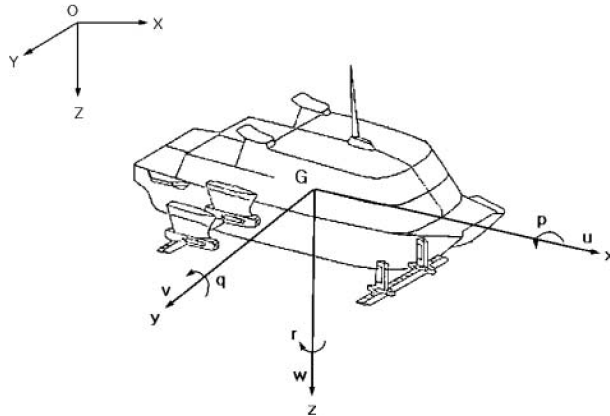


Figure 1. Coordinate system.

In this study, three different control algorithms, PID, linear quadratic regulator (LQR) and sliding mode controls, are applied for the fully submerged hydrofoil model introduced by Kim and Yamato to control longitudinal motion. By comparing the results of all three algorithms, the developed programs are validated and the algorithms are compared. For each wave condition, the characteristics of motion responses are observed, and the simulation results are compared with experimental data in regular waves.

Theoretical background

Equation of motion of fully-submerged hydrofoil ship in waves

Two coordinate systems, space-fixed and body-fixed coordinates as shown in Figure 1, are defined for a fully submerged hydrofoil vessel. Assuming that the centre of the body-fixed coordinate is placed on the mass centre of the vessel, the longitudinal equation of motion can be written as Equations (1) and (2):

$$m\dot{w} - mqU_0 = Z_F + Z_W + Z_C \quad (1)$$

$$I_{yy}\dot{q} = M_F + M_W + M_C. \quad (2)$$

Here, m and I_{yy} are the mass and mass moment of inertia of the vessel about the y axis. w and q are the vertical velocity and the pitch angular velocity. Z stands for the total heave force and M is the total pitch moment. The subscript F means the hydrodynamics force and moment due to the existence of the foil(s). The subscripts W and C indicate wave disturbance and control force.

The vessel dimensions are listed in Table 1. The overall length of the model is 1.5 metres, breadth is 0.6 metres and its mass is 31 kilograms. Two foils are attached in the fore and aft parts of the hull, respectively. The fore foil is positioned 0.5475 metres away from the centre of gravity and the aft foil is positioned 0.3125 metres away. The foils are canard type, therefore the size of the aft foil is larger

Table 1. Dimensions of the model.

| | | | |
|-----------|-------------|-----------|------------|
| Length | 1.5 metre | Breadth | 0.6 metre |
| Mass | 31 kilogram | Foil type | CANARD |
| Fore foil | | | |
| Section | NACA4412 | Depth | 0.35 metre |
| Chord | 0.21 metre | Span | 0.3 metre |
| Aft foil | | | |
| Section | NACA4412 | Depth | 0.35 metre |
| Chord | 0.21 metre | Span | 0.6 metre |

than that of the fore foil. In this model, the span of the aft foil is twice as large as the fore foil. The section of each foil is NACA 4412, and their initial depth is 0.35 metres.

In the motion analysis of typical displacement-type vessels, we take into account Froude–Krylov force, diffraction and radiation forces as wave disturbance. However, in the case of hydrofoil ships, the displacement of the hydrofoil is much smaller than the total displacement of the ship, and lift force and moment are the primary concerns for motion prediction. Therefore it is reasonable to assume that the variation of lift force and moment by the hydrofoil(s) plays a key role in the vessel's motion. In the presence of incident waves, the variation of force and moment is due to the temporal and spatial variation of particle velocity in the wave field, which eventually causes the change of attack angle into the foil(s).

The variation of angle of attack, $\Delta\alpha$, due to the change of water particle velocity in waves, represented as u and w , provides the change of lift force which takes the following form:

$$\Delta L(t) = \frac{1}{2} \cdot \rho \cdot U^2 \cdot S \cdot \frac{dC_L}{d\alpha} \cdot \Delta\alpha. \quad (3)$$

Where $\Delta\alpha = -\tan^{-1}(w/(U + u))$, and ρ , U , S , $dC_L/d\alpha$ are fluid density, the forward speed of vessel, the projected area of the hydrofoil and the variation of lift coefficient per unit angle of attack, respectively. It should be noted that the angle of attack varies in time, since u and w are time-dependent variables.

State-space equation

For the model of Kim and Yamato (2004), the equation of motion is written as the following state-space equation with state variable x and control input variable u :

$$\dot{x} = f(x, u) = Ax + Bu + D. \quad (4)$$

Where,

$$x^T = [z(t), \theta(t), \dot{z}(t), \dot{\theta}(t)], \quad (5)$$

$$u^T = [\delta_f(t), \delta_a(t)], \quad (6)$$

$$A = \begin{bmatrix} 0 & 0 & 1 & 0 \\ 0 & 0 & 0 & 1 \\ 0 & -81.95 & -17.32 & 2.61 \\ 0 & -42.31 & -14.10 & -18.40 \end{bmatrix},$$

$$B = \begin{bmatrix} 0 & 0 \\ 0 & 0 \\ -13.61 & -22.51 \\ 23.39 & -38.31 \end{bmatrix},$$

$$D = \begin{bmatrix} 0 \\ 0 \\ \frac{1}{2}\rho S_{foil}U^2\left(\frac{dC_L}{d\alpha} \cdot \Delta\alpha\right)/m \\ \frac{1}{2}\rho S_{foil}U^2\left(\frac{dC_L}{d\alpha} \cdot \Delta\alpha\right)/I_{yy} \end{bmatrix}. \quad (7)$$

The state variable x is composed of heave motion $z(t)$, pitch motion $\theta(t)$, heave velocity $\dot{z}(t)$ and pitch velocity $\dot{\theta}(t)$. The control input variable u consists of the flap angle of fore and aft hydrofoils. In Equation (7), A matrix stands for the added mass and damping coefficients normalised by mass or mass moment of inertia. B matrix is lift force coefficient, and it is also normalised by mass or mass moment of inertia. Matrix D is the normalised external wave disturbance, which comes from the orbital motion of incident waves.

Control theory

PID control

The proportional–integral–derivative controller is a common feedback loop component. It is a very simple but powerful method; it is known that over 80% of industrial sites use a PID controller. Proportional, integral and derivative controllers can be used in separate or combinational form,

$$u(t) = K_p e(t) + K_i \int e(t)dt + K_d \dot{e}(t). \quad (8)$$

Input signal, i.e. the angle of the foil, $u(t)$ is made of three components as shown in Equation (8), where $e(t)$ is the error vector which means the difference between the actual and desired state variable. K_p , K_i and K_d are the control gains of each controller (Franklin et al. 2006).

LQR control

When a state variable x and an input variable u are defined, a state-space equation can be written as a differential equation like Equation (4). Also a cost function J can be defined with the state variable and input variable:

$$J = \int_0^T (x^T Q x + u^T R u) dt. \quad (9)$$

Where Q and R are the constant non-negative definite matrix and the constant positive-definite matrix that adjust the portion of the state variable and the input variable in the cost function. The goal of LQR control is to find the optimal values which minimise the cost function. The optimal input values can be proportional to the state variable $x(t)$, such that

$$u(t) = -R^{-1} B^T P x(t). \quad (10)$$

Where P matrix indicates a constant matrix which can be obtained from an algebraic Riccati equation (Anderson and Moore 1989):

$$PA + A^T P - PBR^{-1}B^T P + Q = 0. \quad (11)$$

Sliding mode control

An error variable can be obtained from subtracting the desired state variable x_d from the actual state variable x , as follows:

$$e(t) = x_d(t) - x(t). \quad (12)$$

Using this error variable, a sliding surface is defined as Equation (13),

$$s(x, t) = \dot{e}(t) + \lambda e(t). \quad (13)$$

Here $s(x, t)$ is a sliding variable which consists of the error variable and a positive constant λ (Slotine and Sastry 1983). The purpose of using sliding mode control is letting the sliding variable converge to zero. Keeping the sliding vector $s(x, t)$ near the sliding surface where sliding vector is zero can be achieved by adapting sliding condition (14) (Slotine 1984),

$$\frac{1}{2} \frac{d}{dt} s^2 \leq -\eta |s|. \quad (14)$$

Where η is a positive constant that decides the time requirement to make the sliding variable $s(x, t)$ move to zero.

Simulation of motion control

At first, to check the controllability of each scheme and validate the developed program, the vertical motions of the hydrofoil vessel in Table 1 are simulated in regular waves in which experimental data are available. Then, the simulations are carried out extensively to observe the robustness of control algorithms in various wave conditions. In particular, a restriction is assumed in the angle and angular velocity of the flaps in order to impose realistic motion

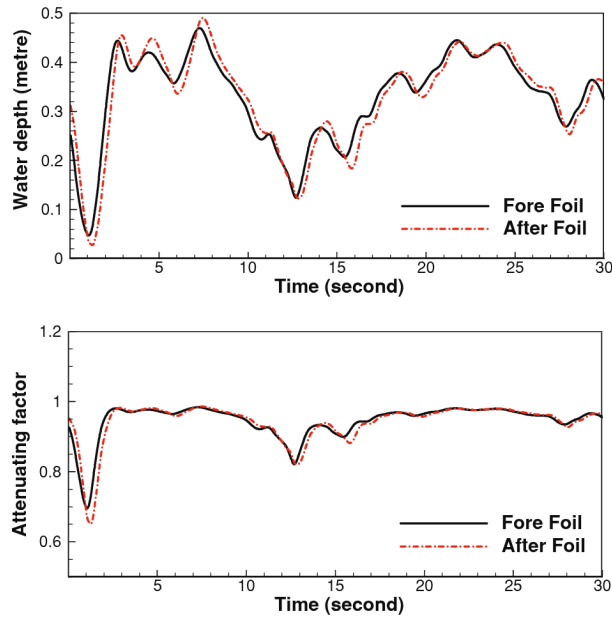


Figure 2. Example of fore and aft foil depths (upper), and corresponding attenuating factors (lower) in irregular waves.

of the hydrofoils. Finally the motion responses in irregular waves are observed.

In the case of regular waves, 3-metre wavelength and 0.05-metre wave height are assumed, as considered by Kim and Yamato (2004). When a hydrofoil gets close to free surface, waves are generated by the hydrofoil itself, and also the lift force on the hydrofoil is influenced by the free surface. In this situation the lift force acting on the hydrofoil becomes generally smaller. In this study, Kaplan's method written as Equation (15) is applied,

$$C_L(d) = C_{L\infty} \left(1 - 0.422 e^{-1.454 d/c}\right). \quad (15)$$

Here, $C_{L\infty}$ is the lift coefficient at infinite water depth, and d and c are the depth and chord of the foil. For instance, Figure 2 shows the depth of hydrofoils and corresponding attenuating factors, obtained in a certain irregular wave condition by adopting PD control. The attenuating factors should be calculated at every time step according to the depth of the foils, and this effect should be included in the equation of motion. In the present vessel, the depths of foils are usually over 0.2 metres, and it means the attenuating factor is normally over 0.9 in motion simulations. At the early stage of the simulation or body motion, this attenuating factor can be less than 0.7 in a short period. Figure 3 compares the heave and pitch motions, corresponding to Figure 2, with and without applying the attenuating factors. This result shows that the effect of attenuation is strong in the early stage of motion control.

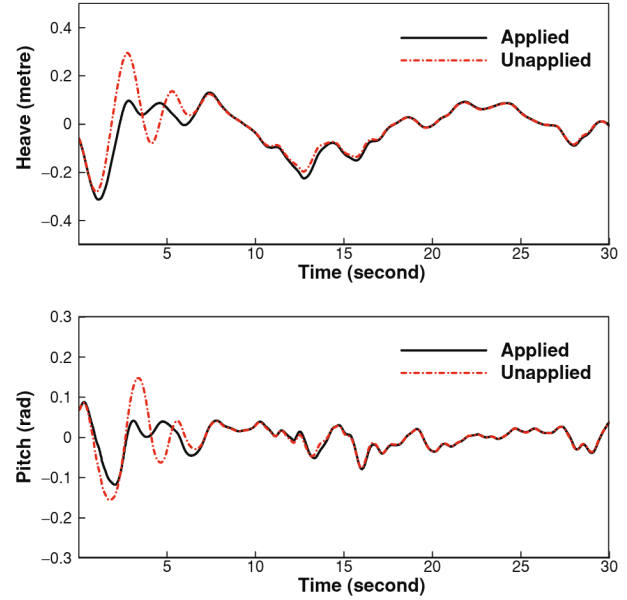


Figure 3. Comparison of heave and pitch motion with and without applying attenuating factors in irregular waves.

Simulation results

Control in regular waves

PID control

Since the PID controller is for single-input and single-output systems, there should be one controller for each hydrofoil. If an identical control input for both hydrofoils is designed, the heave control forces will act in the same direction to the model. This method is very effective in reducing vertical motion in the absence of incident waves. However, in the presence of waves, we need to include the effects of waves disturbance for higher accuracy of motion simulation. This means that a proper phase difference between fore and aft hydrofoils may be needed for more accurate motion control. The angle of attack is affected by particle velocity, and it implies that the wave disturbance varies with the position of the hydrofoil. Hence, there exists a phase difference of lift between the fore and aft foils. When the incident wave properties are known, the wave encounter period and the phase difference between fore and aft foils can be calculated.

Figure 4 shows the motion RAOs and flap-angle RAOs when the ratio of wavelength to foil distance varies from 1.0 to 10.0. It is found that the motion response with 0 degree phase angle between the two foils is easily diverged except for some limited cases. However, the motion becomes much more stable when the phase difference is applied.

A noticeable finding in Figure 4 is that the change of the phase difference to fit the ratio between wavelength and foil distance (marked as 'auto phase' in the legend) provides results worse than the case when the phase difference

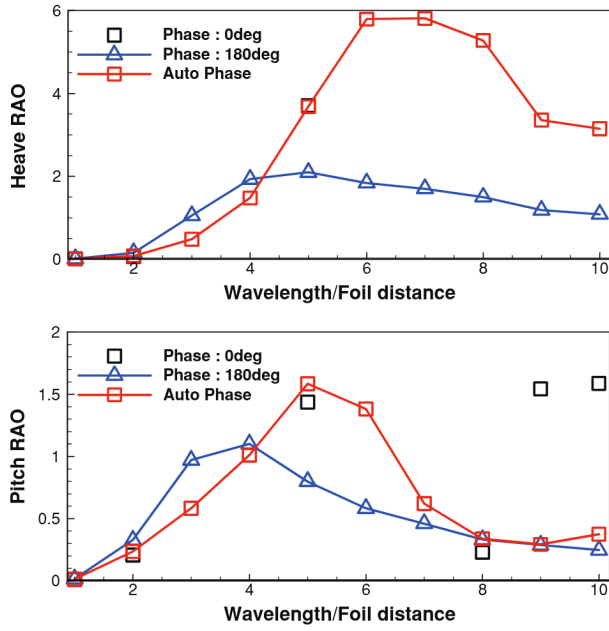


Figure 4. Motion RAOs by PID controller with different phase angles between fore and aft foils.

is fixed to 180 degrees. One of the possible explanations of this unexpected result is related to the error vector for PID control. As mentioned earlier, PID control input is composed of error vectors. The present results are the outputs obtained by using only heave motion for the error vector. Taking pitch motion into the error vector can be considered, however the stability of heave motion can be worse in such a case. Then we can think of the error vector composed of combinations of heave motion, pitch motion, heave velocity and pitch velocity. When this is the case, new variables are involved in the calculation, and it can give rise to the problem of setting the portions between each term. PID control is widely used because of simplicity. However, additional troublesome works make the control system difficult to handle. Another possible reason may be due to the difference in sizes of the considered foils. The experiment model has different sizes of the two spans, different distance between the foils and different locations of mass centre. Therefore, each foil may generate unbalanced heave forces and pitch moments.

LQR control

In LQR control there are control gain matrices, Q and R , described in Equation (9). The Q and R matrices are a constant non-negative definite matrix and a constant positive-definite diagonal matrix. In this study, a very simple case

is chosen to minimise other effort, so the diagonal matrices are chosen as follows:

$$Q = \begin{bmatrix} Q_{11} & 0 & 0 & 0 \\ 0 & Q_{22} & 0 & 0 \\ 0 & 0 & Q_{33} & 0 \\ 0 & 0 & 0 & Q_{44} \end{bmatrix}, \quad R = \begin{bmatrix} R_{11} & 0 \\ 0 & R_{22} \end{bmatrix}. \quad (16)$$

The initial selection of diagonal terms can be based on Bryson's rule (Anderson and Moore 1989). However, since it may not be the optimal cost, a procedure to observe the motion responses for different Q and R matrices is essential.

In this study, a systematic study is carried out to observe the effects of Q and R matrices on the motion control. To this end the ratios: α_1 , α_2 , α_3 , α_4 and α_5 are defined as follows:

$$\begin{aligned} \alpha_1 &= Q_{11}/Q_{33}, \quad \alpha_2 = Q_{22}/Q_{44}, \quad \alpha_3 = Q_{11}/Q_{22}, \\ \alpha_4 &= R_{11}/R_{22}, \quad \alpha_5 = Q_{11}/R_{11}. \end{aligned} \quad (17)$$

In fact, each ratio has own meaning. α_1 means the ratio between heave damping and heave restoring, and α_2 is the ratio between pitch damping and pitch restoring. In addition, α_3 stands for the suppressing balance between heave and pitch. α_4 and α_5 are important ratios related to the balance of the control output between the regulating performance and control energy (Lee and Rhee 2002). In this paper a lot of test cases listed in Table 2 are applied for motion simulation, and the heave motion, pitch motion and control inputs are compared.

Case 6 is the set of gains which was used in Kim and Yamato's experiments. According to our observation, Case 6 provides better results in motion control, i.e. smaller motion RAOs, except for cases 9, 10 and 11. Figures 5 and 6 show the time histories of motion signal and flap angle for cases 6, 9, 10 and 11. In the present cases, the motion response becomes regular after about 5 seconds from the motion start. It should be mentioned that, during transient motion before 5 seconds, case 6 provides smoother transient motion than any other case. Furthermore, as Figure 6 shows, the flap angle in case 6 changes very naturally, while the flap angles of the other cases change quickly in a saw-tooth manner. Based on this observation, the set of control gain matrices are finally chosen as Equations (18),

$$\begin{aligned} Q &= \begin{bmatrix} 50 & 0 & 0 & 0 \\ 0 & 10 & 0 & 0 \\ 0 & 0 & 1 & 0 \\ 0 & 0 & 0 & 10 \end{bmatrix}, \quad R = \begin{bmatrix} 100 & 0 \\ 0 & 100 \end{bmatrix}, \\ K &= \begin{bmatrix} -0.69 & 1.42 & -0.07 & 0.12 \\ 0.15 & -0.73 & 0.03 & -0.11 \end{bmatrix}. \end{aligned} \quad (18)$$

Table 2. Test cases for α_i .

| Case | 1 | 2 | 3 | 4 | 5 | 6 | 7 | 8 | 9 | 10 | 11 |
|------------|-----|-----|-----|-----|-----|-----|------|-----|-----|-----|------|
| α_1 | 50 | 50 | 5 | 50 | 5 | 50 | 5 | 5 | 5 | 5 | 5 |
| α_2 | 1 | 10 | 1 | 0.1 | 0.1 | 1 | 0.1 | 0.1 | 0.1 | 0.1 | 0.01 |
| α_3 | 50 | 5 | 50 | 50 | 50 | 5 | 50 | 50 | 50 | 50 | 500 |
| α_4 | 1 | 1 | 1 | 1 | 1 | 1 | 2 | 2 | 1 | 1 | 1 |
| α_5 | 0.5 | 0.5 | 0.5 | 0.5 | 0.5 | 0.5 | 0.25 | 0.5 | 1 | 2 | 1 |

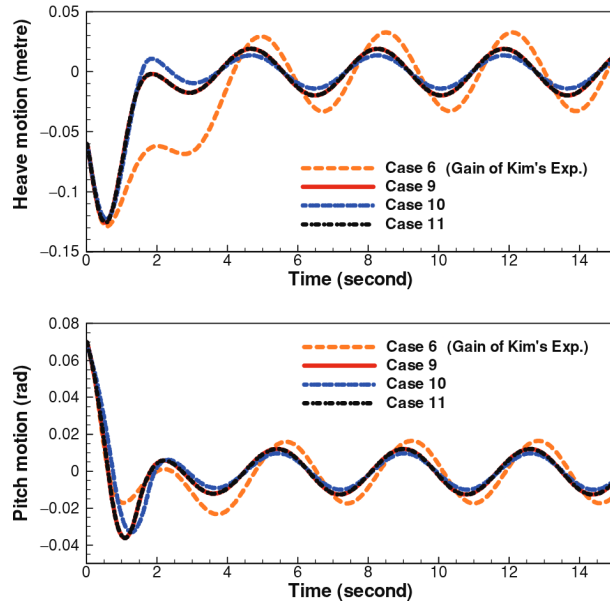


Figure 5. Motion signals of the selected cases (upper: heave, low: pitch).

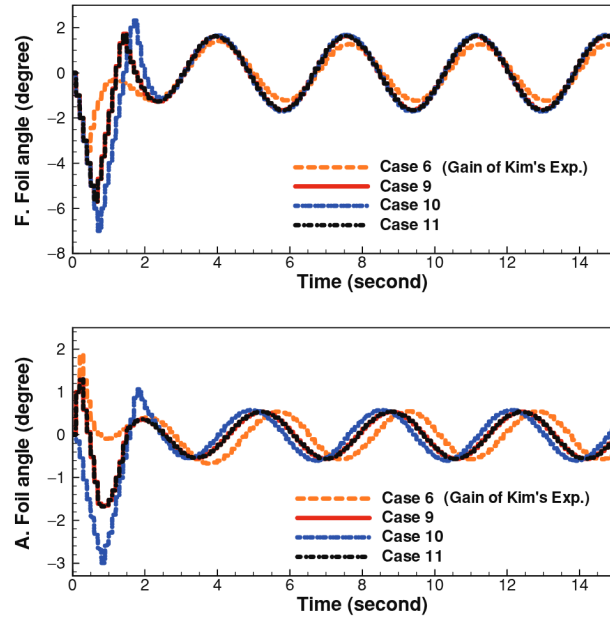


Figure 6. Flap-angle signals of the selected cases (upper: fore foil, low: aft foil).

Sliding mode control

Figures 7 and 8 show the motion signal and flap angle signal, controlled by the sliding mode control algorithm. In general, the performance of the sliding mode control can become poor when the sliding variable becomes very small. When this is the case, to increase the efficiency of the performance, the sign function $sgn(s(t))$ instead of sliding variable $s(t)$ is applied. In Figures 7 and 8, motion control using $sgn(s(t))$ provides better performance than by using $s(t)$. However, using $sgn(s(t))$ causes a side effect, resulting in a chattering problem due to the discontinuity of the sign function (Perruquetti and Barbot 2002). To remove this phenomenon, the saturation function is applied in the present study. The saturation function takes a proportional value to the sliding variable in a small range between $-\varepsilon$ and ε (a small positive constant). The slope of the linear portion of $sat(s/\varepsilon)$ is $1/\varepsilon$, and good approximation requires the use of small ε (Khalil 2002).

Figures 7 and 8 include the simulation result when the saturation function is applied. The chattering problem in flap angle is obvious from about 10 seconds when $sgn(s(t))$

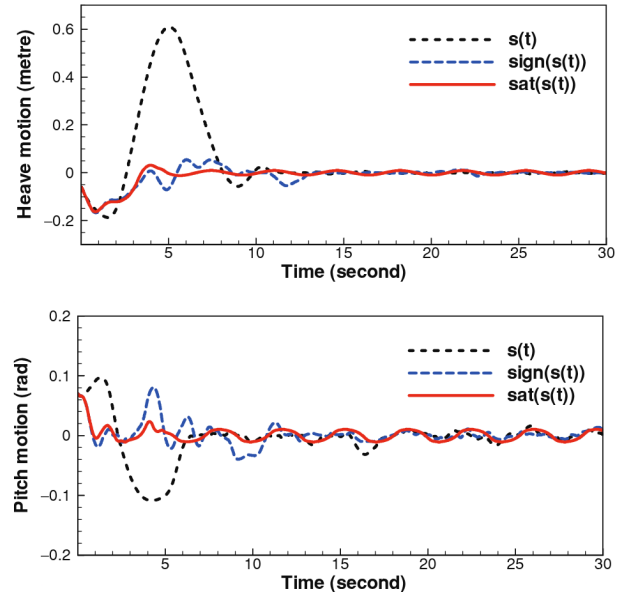


Figure 7. Motion responses simulated by using sliding mode control.

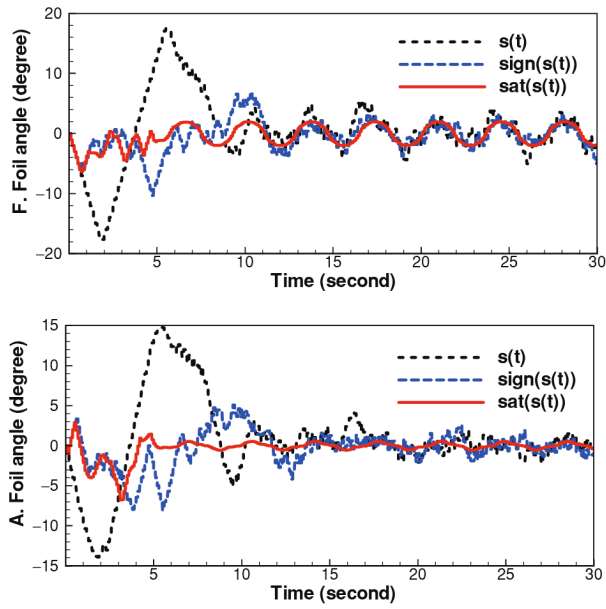


Figure 8. Signals of flap angle during the application of sliding motion control.

is applied. However, it is also clear that the application of the saturation function can be a good remedy for such a problem.

Comparison with the experiment results

Figures 9 and 10 show the comparison between the present simulation results and experimental data. The experiment was carried out by Kim and Yamato (2004) with the application of LQR control and Karman filter. For a fair comparison, the same control inputs are used in the present simulation.

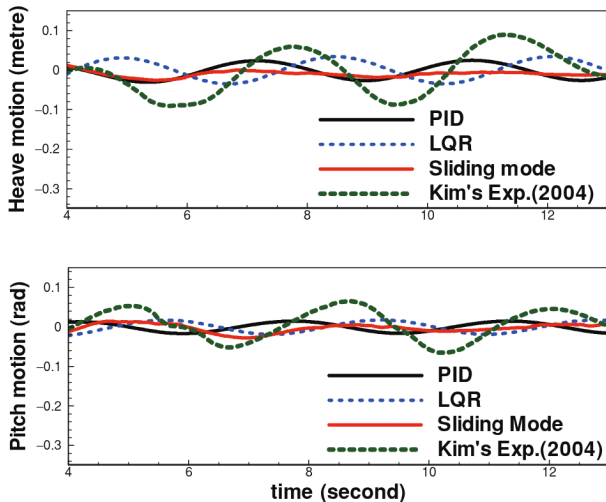


Figure 9. Comparison of motion responses with experimental results in regular waves.

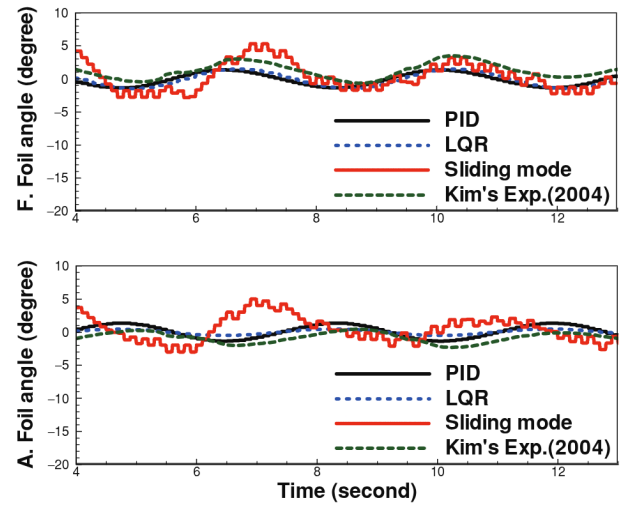


Figure 10. Comparison of flap angle with experimental results in regular waves.

The overall results of the simulation are a little smaller than the experimental results. This trend is natural since, in the experiment, disturbances acting on the model include not only the change of lift force due to the angle of attack but also wave diffraction forces, viscous effects, non-linear effects and so on. Therefore, theoretical simulation predicts better performance, which is not actually true in the real situation.

Among the three algorithms, the sliding mode control provides the best performance of the motion control, but requires the largest control input and the rate of change. These are the particular characteristics of the sliding mode control, mentioned above.

Robustness in various wave environments

To ascertain the robustness in various wave conditions, the control algorithms are applied for different wavelengths and wave heights, and the resultant motions and control inputs are compared.

The typical time history of a motion signal can be divided into a transient part and a quasi-state part. However, in the observation of actual signals, it is hard to define at which time the signal becomes quasi-state. In the present study, a 60-second time window is considered for each case; the first half is considered to be the transient part and the second half is the quasi-state part. The root-mean-square (RMS) values of those two parts are computed at each simulation run, and their quantities are compared. The motion RAO has been a parameter to characterise the motion property, but RMS seems a more appropriate parameter for the present comparison, since it is not suitable for the transient part.

Robustness to wavelength

To check the effects of wavelength, the ratio of wavelength to the ship length is varied from 0.5 to 3. Wave height and the

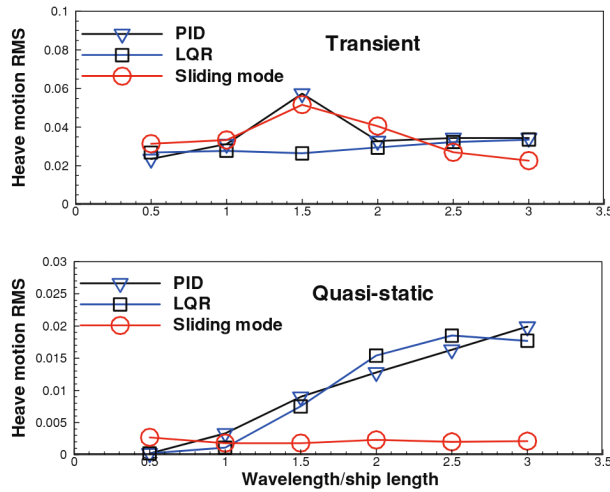


Figure 11. Heave RMS with various wavelengths.

vessel speed are fixed at 0.05 metres and 3 metres/second, respectively. The simulation results are summarised in Figures 11 and 12.

It is found that the transient heave motions of PID and sliding mode controls are somewhat large at the ratio 1.5, while LQR control provides the more stable transient heave motions through all the wavelengths. In the quasi-static heave motions, RMS values tend to increase according to the wavelength except for sliding mode control. In particular, the sliding mode control shows a remarkable performance in reducing quasi-static heave motions. However, pitch motion does not show the same tendency. Both the LQR and sliding mode control algorithms show similar performance during transition, but not in quasi-static conditions.

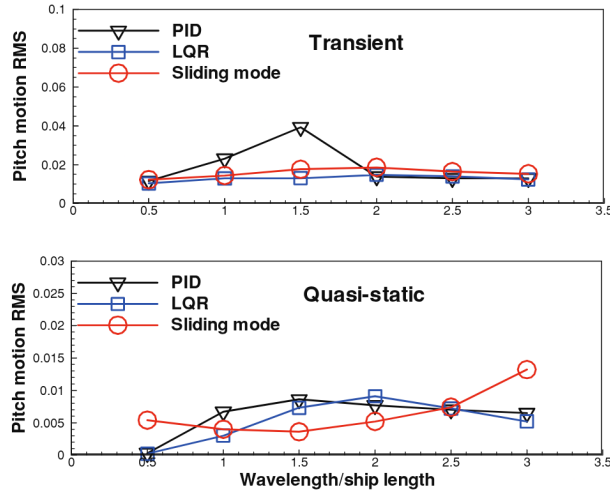


Figure 12. Pitch RMS with various wavelengths.

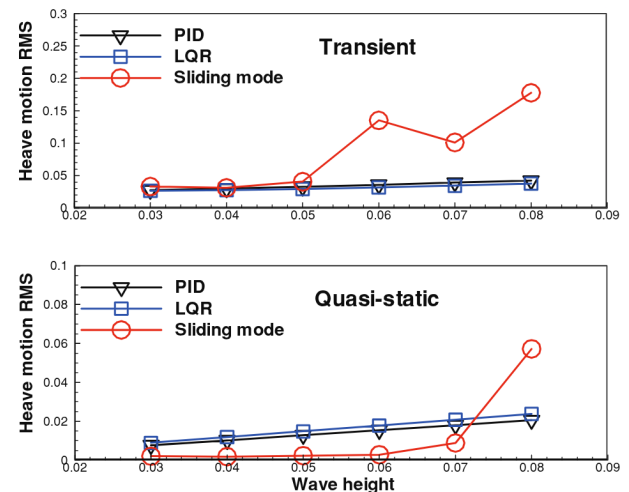


Figure 13. Heave RMS with various wave heights.

Robustness to wave height

In this test, wave height is changed from 0.03 to 0.08 metres, corresponding to the ratio of wave height to ship length from 0.02 to 0.533. Wavelength and ship speed are fixed to 3 metres and 3 metres/second. Control gains are fixed in all the cases, and the gains for the wave height–ship length ratio of 0.033 are chosen. The simulation results are plotted in Figures 13 and 14.

As can easily be seen, larger motion RMS can be observed at larger wave height. Naturally, this tendency is more clear in the quasi-static motion than the transient motion. Another finding is that sliding mode control provides a trend somewhat different from the other two algorithms. When the ratio of wave height to the ship length is less than 0.04, the quasi-static motions are nearly zero. However, when the ratio is over 0.04, the motion becomes larger than any other results. It implies that sliding mode control

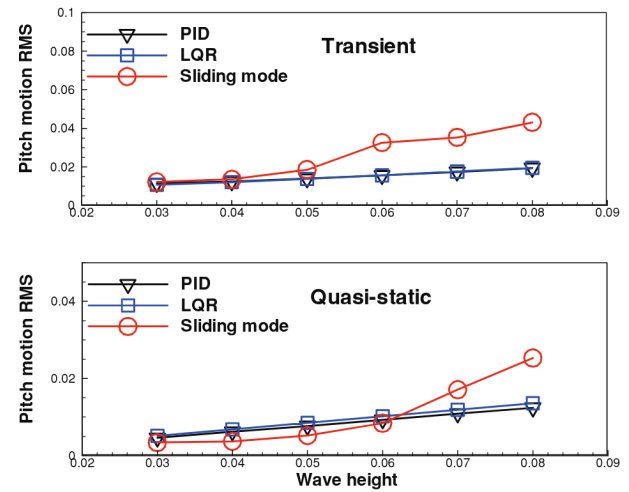


Figure 14. Pitch RMS with various wave heights.

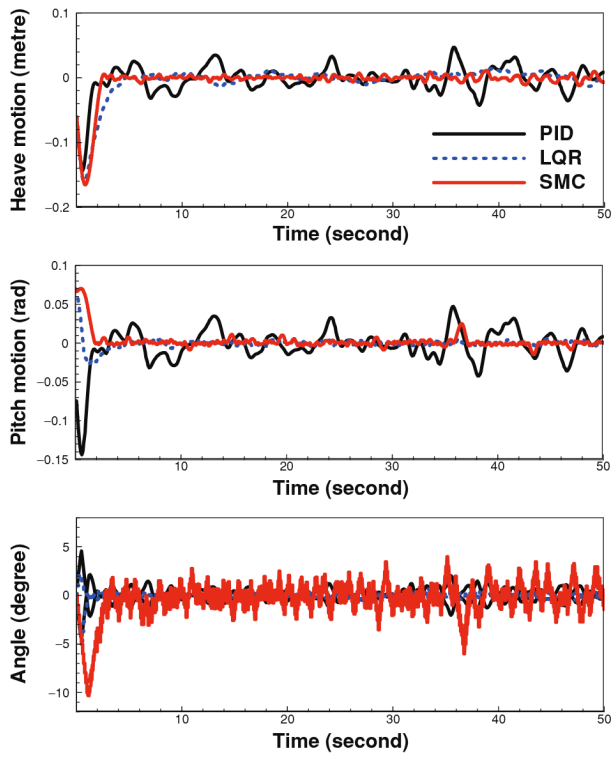


Figure 15. Motion signal and control input in irregular waves: heave motion (upper), pitch motion (middle), and control input (lower), non-dimensional significant wave height and mean wave period are 0.67 and 1.25.

can be sensitive to wave height, and this may come from the control gains, which are fixed in these cases. By changing the control gains better performance can be expected.

Control in irregular waves

The present study is extended to motion control for irregular wave conditions. To generate irregular waves, the ITTC spectrum is equally discretised into 200 components within 2% error of wave energy.

The controlled motions in irregular waves are presented in Figure 15. In this simulation, the significant wave height and mean wave period normalised with respect to the ship length are 0.67 and 1.25, respectively. In the case of PID control, it is observed that transient motion does not decay quickly when the proportional gain is large, and the derivative controller reacts sensitively to the change rate of wave disturbance when the derivative gain is large. Even though PID control is effective in attenuating the motions to some extent, it is observed that the motion is more unstable than the other control algorithms.

For heave motion, LQR and the sliding mode controls provide similar performance, but the motion of sliding mode control is slightly bigger. As in regular waves, it is observed that the control inputs of sliding mode control are larger than those of LQR and PID controls. The output of

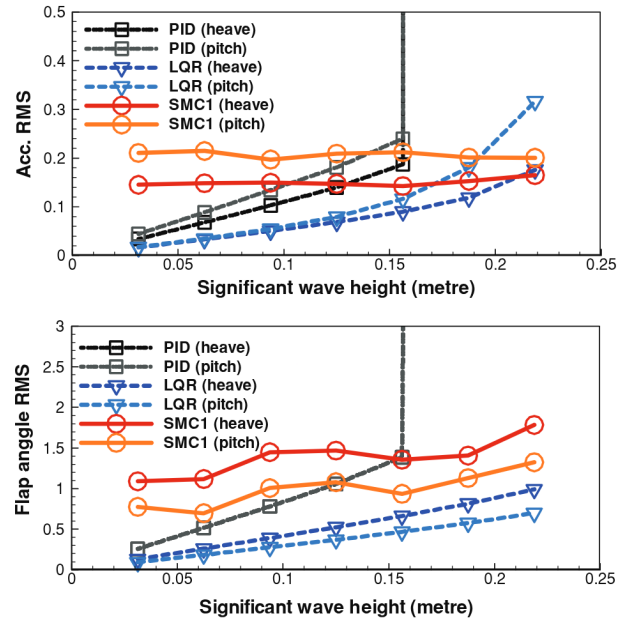


Figure 16. RMS values of vertical accelerations and flap angle in irregular waves for various significant wave heights.

LQR control shows the most stable motion signals in the considered irregular waves. No excessive motion is found in all the simulations, and the control inputs are less than 1 degree after transient motion.

Figure 16 summarises the RMS values of vertical acceleration and flap angle in a range of significant wave heights—ship length ratio from 0.1667 to 0.8333. Similar to the regular wave cases, the acceleration grows in proportion to significant wave height when PID and LQR are applied. The result of PID control shows strong sensitivity to significant wave height, and the motion diverges when the ratio of significant wave height to the ship length is over 0.8333. It is obvious that the control inputs and accelerations of LQR control are more stable than any other algorithm. In the case of sliding mode control, the performance of motion response is good but jagging of the motion signal (see the bottom figure of Figure 15) results in large RMS values of acceleration.

One possible reason for the larger acceleration at higher-amplitude waves is due to the restriction of the hydrofoil actions. We imposed a certain restriction on the flap angle, and this restriction should work differently at different wave conditions. Another possible reason is due to the attenuation factor near free surface. When the hydrofoils are close to free surface, lift force becomes less owing to free surface effects. Then this effect can be different at different wave amplitudes.

Conclusions

In the present paper, the three control algorithms, PID, LQR and sliding mode controls, are applied for controlling the

longitudinal motion of a fully-submerged hydrofoil vessel. Some key findings are as follows:

- PID control gives a good overall performance in regular waves, but it is observed that the sensitivity to wave height is strong in irregular waves, even causing instability in large waves. This is due to the derivative controller that responds sensitively to the rapid change of disturbance in irregular waves.
- It is reconfirmed that LQR control shows an excellent performance in various wave environments include regular and irregular waves. This algorithm attenuates the motion effectively with small control inputs.
- Sliding mode control provides the most reduction of quasi-static motion in the particular cases that exact wave disturbance is given. However, when wave disturbance data is not accurate or not provided, the motion easily tends to be unstable. Furthermore, to be effective to reduce motions in waves, it requires bigger flap angle of hydrofoils than LQR control.

Acknowledgements

Authors appreciate Prof. S.H. Kim for providing experimental data, and Prof. H.J. Kim for technical advice and assistance. Authors also thank the administrative support of RIMSE and ERI of Seoul National University.

References

Anderson BDO, Moore JB. 1989. Optimal control: linear quadratic methods. Prentice Hall: Englewood Cliffs, NJ, USA.

- Chatzakis I, Sclavounos PD. 2006. Active motion control of high-speed hydrofoil vessels by state-space methods. *J Ship Res.* 50(1):49–62.
- Franklin GF, Powell JD, Emami-Naeini A. 2006. Feedback control of dynamic systems. Pearson Prentice Hall: Englewood Cliffs, NJ, USA.
- Kang C-G, Hong S-Y, Suh S-H, Lee C-M, Lim Y-G, Gong I-Y. 1993. Attitude control system for a high speed catamaran with hydrofoils in waves. *Proc. the Second International Conference on Fast Sea Transportation*, Yokohama, Japan.
- Khalil HK. 2002. Nonlinear systems. Prentice Hall: Englewood Cliffs, NJ, USA.
- Kim J-K. 1997. Development of attitude control system for high-speed foil-assisted catamaran considering modeling uncertainties [PhD Thesis]. Seoul National University, Seoul, Korea.
- Kim S-H, Yamato H. 2004. An experimental study of the longitudinal motion control of a fully submerged hydrofoil model in following seas. *Ocean Eng.* 31:523–537.
- Kim S-H, Yamato H. 2005. The estimation of wave elevation and wave disturbance caused by the wave orbital motion of a fully submerged hydrofoil craft. *J Marine Sci Technol.* 10(1):22–31.
- Lee S-Y, Rhee K-P. 2002. Design of ship motion regulators for foil catamaran in irregular sea waves. *IEEE J Oceanic Eng.* 27(3):738–752.
- Perruquetti W, Barbot JP. 2002. Sliding mode control in engineering. Marcel Dekker: New York, NY, USA.
- Slotine JJ. 1984. Sliding controller design for nonlinear systems. *Int J Control.* 40(2):421–434.
- Slotine JJ, Sastry SS. 1983. Tracking control of nonlinear systems using sliding surfaces, with application to robot manipulators. *Int J Control.* 38(2):465–492.
- Ulusoy T. 2006. State-space modeling and optimal control of ship motions in a seastate [PhD Thesis]. Massachusetts Institute of Technology, Cambridge, MA, USA.